Accepted Manuscript

Lipid metabolism alterations in the neuronal response to A53T α-synuclein and Fe-induced injury

Sánchez Sofía Campos, Natalia P. Alza, Gabriela A. Salvador

PII: S0003-9861(17)30740-3

DOI: 10.1016/j.abb.2018.08.007

Reference: YABBI 7794

To appear in: *Archives of Biochemistry and Biophysics*

Received Date: 2 November 2017

Revised Date: 3 August 2018

Accepted Date: 8 August 2018

Please cite this article as: Sá.Sofí. Campos, N.P. Alza, G.A. Salvador, Lipid metabolism alterations in the neuronal response to A53T α-synuclein and Fe-induced injury, *Archives of Biochemistry and Biophysics* (2018), doi: 10.1016/j.abb.2018.08.007.

Figure 7

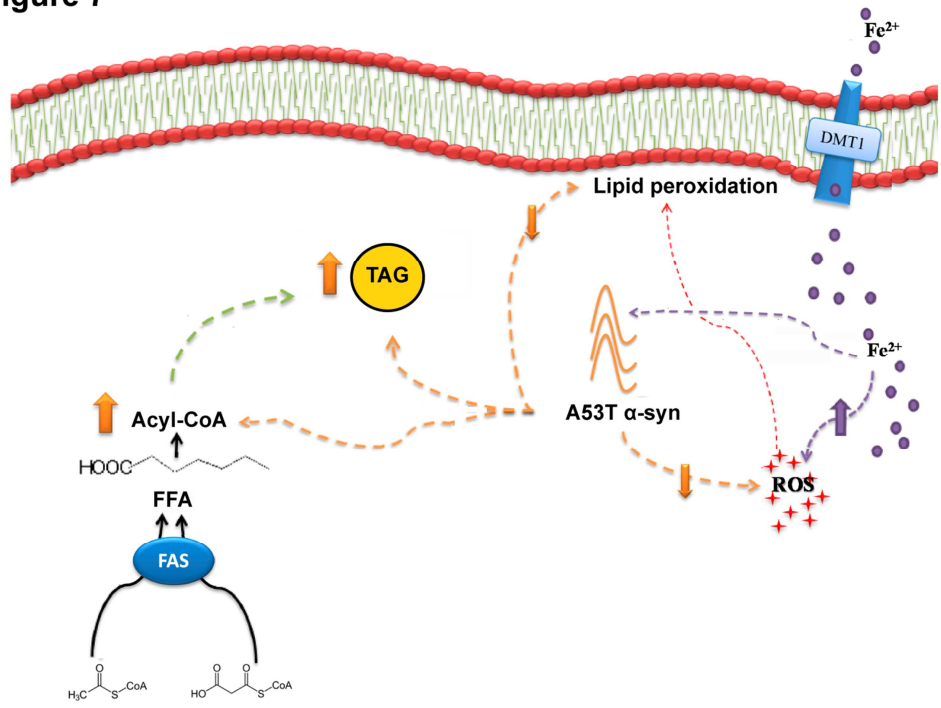

Lipid metabolism alterations in the neuronal response to A53T α-synuclein and Fe-induced injury

Sánchez Campos Sofía[1,2], Alza Natalia P.[1,3] and Salvador Gabriela A.[1,2]✉

[1]Instituto de Investigaciones Bioquímicas de Bahía Blanca (INIBIBB)- Consejo Nacional de Investigaciones Científicas y Técnicas (CONICET), [2] Departamento de Biología Bioquímica y Farmacia -Universidad Nacional del Sur (UNS) and [3] Departamento de Química UNS, Bahía Blanca, Argentina.

Running title: A53T α-synuclein, neuronal injury and lipid metabolism

Keywords: dopaminergic neurons, A53T α-synuclein, iron, oxidative stress, triacylglycerol, lipid metabolism.

✉**To whom correspondence should be addressed:** Gabriela A. Salvador, Instituto de Investigaciones Bioquímicas de Bahía Blanca, La Carrindanga Km 7, 8000 Bahía Blanca, Buenos Aires, Argentina. Tel.: +54-291-4861201. Fax: +54-291-4861200. E-mail: salvador@criba.edu.ar.

HIGHLIGHTS

A53T α-syn overexpression induced TAG and lipid droplet accumulation in dopaminergic neurons.

Dopaminergic neurons that overexpressed A53T α-syn displayed augmented Acyl-CoA synthetase activity.

Fe induced A53T α-syn aggregation and increased TAG content in neurons.

Blockage of TAG synthesis reduced A53T α-syn cell viability.

ABBREVIATIONS

The abbreviations used in this study are: **ACS**, Acyl-CoA synthetase; **α-syn**, α-synuclein; **A53T α-syn cells**, N27 neurons expressing the vector pcDNA3-A53T α-synuclein; **BSA**, bovine serum albumin; **Chol**, cholesterol; **DCDCDHF**, dichlorodihydrofluorescein diacetate; **DAG**, diacylglycerols; **DTT**, dithiothreitol; **EDTA**, N,N'-1,2-ethandiylbis[N-(carboxymethyl)glycine] disodium salt; **FA**, fatty acid; **FAME**, fatty acid methyl esters; **FAS**, fatty acid synthase; **FBS**, fetal bovine serum; **FFA**, free fatty acid; **GC**, gas-liquid chromatography; **HRP**, horseradish peroxidase; **LDH**, lactate dehydrogenase; **MAG**, monoacylglycerol; **MTT**, 3-(4,5-dimethylthiazol-2-yl)-2,5 diphenyltetrazolium bromide; **OA,** Oleic acid; **OS**, oxidative stress; **PBS**, phosphate buffer saline; **pcDNA cells**, N27 neurons expressing the empty vector pcDNA3; **PD**, Parkinson's disease; **PL**, phospholipids; **PMSF**, phenylmethylsulfonyl fluoride; **ROS**, reactive oxygen species; **SDS**, sodium dodecyl sulphate; **SDS–PAGE**, sodium dodecyl sulphate-polyacrylmide gel electrophoresis; **TAG**, triacylglycerols; **TBA**, thiobarbituric acid; **TBARS**, thiobarbituric acid reactive substances; **TBS-T**, Tween-Tris Buffer Saline; **UT**, untransfected neurons.

Abstract

Pathological α-synuclein (α-syn) overexpression and iron (Fe)-induced oxidative stress (OS) are involved in the death of dopaminergic neurons in Parkinson's disease (PD). We have previously characterized the role of triacylglycerol (TAG) formation in the neuronal response to Fe-induced OS. In this work we characterize the role of the α-syn variant A53T during Fe-induced injury and investigate whether lipid metabolism has implications for neuronal fate. To this end, we used the N27 dopaminergic neuronal cell line either untransfected (UT) or stably transfected with pcDNA3 vector (as a transfection control) or pcDNA-A53T-α-syn (A53T α-syn). The overexpression of A53T α-syn triggered an increase in TAG content mainly due to the activation of Acyl-CoA synthetase. Since fatty acid (FA) β-oxidation and phospholipid content did not change in A53T α-syn cells, the unique consequence of the increase in FA-CoA derivatives was their acylation in TAG moieties.

Control cells exposed to Fe-induced injury displayed increased OS markers and TAG content. Intriguingly, Fe exposure in A53T α-syn cells promoted a decrease in OS markers accompanied by α-syn aggregation and elevated TAG content.

We report here new evidence of a differential role played by A53T α-syn in neuronal lipid metabolism as related to the neuronal response to OS.

1. Introduction

Parkinson's disease (PD) is associated with movement disorders and is the second most common age-related neurodegenerative disorder after Alzheimer's disease. PD is a multifactorial and complex disorder including epidemiological, genetic and toxicological factors whose main cause is the progressive loss of dopaminergic neurons [1]. One of the most studied events in the neurodegeneration of the *substantia nigra* is the overexpression and pathological aggregation of α-synuclein (α-syn) [1,2]. The role of α-syn in the ethiopathogenesis of PD is supported by *post-mortem* studies showing pathognomonic intracellular inclusions of this protein in the *substantia nigra*, known as Lewy bodies [3,4]. *In vivo* studies in transgenic mice highlight the involvement of α-syn overexpression (wild type and mutated forms) in the development of neurobiological and behavioral impairment [3,5,6]. Genome-wide association studies demonstrated several genetic variants for the α-syn (SNCA) locus related to idiopathic and inherited forms of PD, among which A53T α-syn, one of the most common variants, generated by aminoacid substitution, is present in young onset PD [7–9]. Despite numerous studies on the subject, the physiological role and pathological mechanism triggered by α-syn and its variants are not yet clear.

One of the most intriguing questions regarding α-syn function is its relationship with lipid metabolism. Mounting evidence indicates that α-syn overexpression alters neuronal and brain phospholipid (PL) levels and also fatty acid (FA) composition [10–13]. α-syn is also able to bind lipid bodies (containing triacylglycerol-TAG- and cholesterol-chol-), FA and PL [14–16]. We have recently reported that overexpression of wild-type α-syn downregulates phospholipase D1 and impacts on neuronal cytoskeleton [17].

Another important triggering factor for the onset and progression of PD besides α-syn is iron (Fe) accumulation and in consequence, elevated levels of oxidative stress (OS) [18]. In this connection, ferrireductase activity has been attributed to α-syn, which thus participates in the redox reaction yielding Fe^{2+} from Fe^{3+} [19,20]. A53T α-syn has been shown to autoaggregate in the presence of Fe and iron chelation is able to revert pathological metal/α-syn interactions [9,21–23]. This cumulative evidence points to a link between A53T α-syn, lipid metabolism and Fe-induced neuronal damage in PD.

We have previously demonstrated that during Fe-induced OS, dopaminergic neurons respond by modulating lipid acylation and TAG accumulation [24]. Based on the above data, our aim was to study the role of A53T α-syn in neuronal lipid metabolism during Fe-induced injury. To this end, N27 dopaminergic cells stably expressing A53T α-syn (A53T α-syn) were exposed to Fe and the state of lipid metabolism and cellular oxidative damage evaluated.

2. Materials and Methods

2.1. Materials

Triton X-100, 3-(4,5-dimethylthiazol-2-yl)-2,5 diphenyltetrazolium bromide (MTT), thiobarbituric acid (TBA), Thioflavin S, DL-Propranolol hydrochloride, Oil Red O, Malonyl-CoA and Triacsin C were obtained from Sigma-Aldrich (St. Louis, MO, USA). DCDCDHF, Hoechst and DAPI were obtained from Molecular Probes (Eugene, Oreg., USA). Ferrous sulphate (J.T.Baker, cat.# 2070-01) and polyvinylidene difluoride membranes were obtained from EMD Millipore (Millipore, Bedford, MA). Antibodies:

rabbit polyclonal anti-α-synuclein (C-20-R) [sc-7011-R], mouse monoclonal anti-fatty acid synthase (FAS) (G-11) [sc48357], anti-tyrosine hydroxylase (TH) (F-11) [sc-25269], goat polyclonal anti-actin (C-11) [sc 1615], polyclonal horseradish peroxidase (HRP)-conjugated goat anti-rabbit IgG, polyclonal HRP-conjugated goat anti-mouse IgG, polyclonal HRP-conjugated bovine anti-goat IgG, cerulenin and geneticin (G418) were purchased from Santa Cruz Biotechnology, Inc. (Santa Cruz, CA, USA). Fetal bovine serum (FBS) was obtained from Natocor (Córdoba, ARG). RPMI 1640 medium was obtained from Gibco (USA). LDH-P UV AA kit was kindly provided by Wiener Lab Group (CABA, Bs As, ARG). TG color GPO/PAP AA and enzymatic Colestat were purchased from Wiener lab Group. [^{3}H]-oleic acid (OA) and [^{3}H]-glycerol were obtained from Perkin-Elmer (Migliore-Laclaustra, CABA, Bs As, ARG). All other chemicals used in the present study were of the highest purity available.

2.2. Methods

2.2.1. Cell culture and stable expression of α-syn

The immortalized rat mesencephalic dopaminergic cell line 1RB3AN27, also referred to as N27 cells, was kindly donated by Dr. Patricia Oteiza (Department of Nutrition, UC DAVIS). Cells were grown in RPMI 1640 medium supplemented with 10 % (v/v) FBS, 100 U/ml penicillin, 100 µg/ml streptomycin and 0.25 µg/ml amphotericin B in a humidified atmosphere of 5 % CO_2 at 37°C. Dr. Benjamin Wolozin (Boston University) kindly provided the pcDNA3-A53T-α-syn expression vector containing the mutated full-length human α-syn sequence. pcDNA3-A53T-α-syn or pcDNA3 were transfected into N27 cells using Lipofectamine 2000 reagent (Invitrogen, CABA, Bs. As., ARG) following the procedure recommended by the manufacturer. The polyclonal stable transfected cells were

selected 48 h post-transfection in 400 µg/ml of geneticin (G418) and further maintained in N27 growth media supplemented with 200 µg/ml of G418. Expression levels of α-syn were confirmed by immunocytochemistry.

2.2.2. Experimental treatments

In all the experiments carried out, cells were grown to 80%-90% confluence. Fe treatments were carried out in serum-free medium. Treatments with inhibitors were performed as follows: medium was removed and replaced with serum-free media. Inhibitors were subsequently added to the desired final concentration (100 µM DL-Propranolol, 5 µM Triacsin C, 5-10 µg/ml Cerulenin and 0.1-10 µM Malonyl-CoA); controls received vehicle alone (0.02% ethanol, water, 0.015% methanol or 0.05% DMSO). In the experiments of Fe exposure, after 30 min, 1 mM Fe ($FeSO_4$) or its vehicle (ultrapure water) was added and cells were incubated under these conditions for 24 h unless otherwise specified.

2.2.3. Immunofluorescence microscopy

N27 cells were grown onto glass coverslips and the growing medium was replaced by serum-free medium [24]. After treatments, cells were fixed for 1 h with 4% paraformaldehyde in PBS, followed by permeation with Triton X-100 (0.1%) for 15 min. For the immunostaining, the non-specific sites were blocked with 2% bovine serum albumin (BSA) in PBS at room temperature for 30 min. Cells were incubated with anti α-syn (1:100 in PBS, 2% BSA) or anti -TH (1:50 in PBS, 2% BSA) for 1 h at room temperature. After three washes with PBS, cells were incubated with Alexa Fluor® 546-conjugated secondary antibody (1:200, 1 h, room temperature) and Hoechst or DAPI for nuclear staining. After washing with PBS, coverslips were mounted and slides were observed with a Nikon Eclipse E-600 microscope. Quantification was performed using

ImageJ (a freely available application in the public domain for image analysis and processing, developed and maintained by Wayne Rasband at the Research Services Branch, National Institute of Health, Bethesda, MD, USA) and at least 100 cells for each condition were analyzed from two independent cell cultures.

2.2.4. Triacylglycerol and cholesterol measurement

After treatments, cells were washed 3 times with PBS, scraped off and subjected to lipid extraction following the method of Bligh and Dyer [25]. Lipid extracts were washed twice with Bligh and Dyer upper phase, dried under N_2, resuspended in chloroform/methanol (2:1, v/v) and spotted on silica gel plates. For the resolution of neutral lipids, silica gel G plates were used; the mobile phase consisted of hexane: diethylether (80:20, v/v). After separation by TLC, the spots corresponding to TAG and chol were scraped off the silica and eluted [24]. Total TAG and chol content were measured in aliquots of the lipid extracts corresponding to 10 µg lipid P, using commercial kits (TG color GPO/PAP AA and enzymatic Colestat). Aliquots were dried under N_2 gas and resuspended in 100 µl of isopropanol and TAG and cholesterol determination were performed following the manufacturer's instructions.

2.2.5. Lipid phosphorus measurement

Lipid phosphorus (lipid P) was determined in total lipid extracts using the chemicals and reactions described by Rouser and collaborators [26].

2.2.6. Assessment of cell viability

Cell viability was assessed by MTT reduction assay. MTT is a water-soluble tetrazolium salt that is reduced by metabolically viable cells to a colored, water insoluble formazan salt.

After treatments, MTT (5 mg/ml) was added to the cell culture medium at a final concentration of 0.5 mg/ml. After incubating the plates for 2 h at 37ºC in a 5 % CO_2 atmosphere, the assay was stopped and the MTT-containing medium was replaced with solubilization buffer (20 % SDS, pH 4.7). The extent of MTT reduction was measured spectrophotometrically at 570 nm [24]. Results are expressed as a percentage of the control.

2.2.7. Oil Red O staining

For lipid droplet staining, the Oil Red O method was used as described by Bi *et al.* 2012 [27] with slight modifications. Cells were grown and fixed as described in 2.2.3. After three washes with PBS and one wash with water, cells were incubated with a freshly prepared solution of Oil Red O (570 µl of 0.5% Oil Red O in isopropanol and 380 µl of water) for 1 h. Cells were then rinsed thoroughly with water and nuclei were stained with DAPI. Samples were mounted and analyzed in the fluorescence microscope.

2.2.8. Western blot analysis

For the preparation of total cell extracts, cells (10×10^6 cells) were rinsed with PBS, scraped and centrifuged. The pellet was rinsed with PBS and resuspended in 80 µl of a buffer containing 50 mM Tris, pH 7.5, 150 mM NaCl, 0.1 % Triton X-100, 1 % NP-40, 2 mM EDTA, 2 mM EGTA, 50 mM NaF, 2 mM β-glycerophosphate, 1 mM Na_3VO_4, 10 µg/ml leupeptin, 5 µg/ml aprotinin, 1 µg/ml pepstatin, 0.5 mM PMSF, and 0.5 mM DTT. Samples were exposed to one cycle of freezing and thawing, incubated at 4 °C for 60 min and centrifuged at 10000 x g for 20 min. The supernatant was decanted and the protein concentration was measured [28]. Cell lysates containing 25–50 µg of protein were separated by reducing 7–12.5% polyacrylamide gel electrophoresis and electroblotted to polyvinylidene difluoride membranes. Molecular weight standards (Spectra™ Multicolor

Broad Range Protein Ladder, Thermo Scientific) were run simultaneously. Membranes were blocked with 5 % nonfat dry milk in TBS-T buffer (20 mM Tris-HCl [pH 7.4], 100 mM NaCl, and 0.1 % [wt/vol] Tween 20) for 1 h at room temperature and subsequently incubated overnight at 4 ºC with primary antibody (anti-FAS (G-11): sc-48357, anti-α-syn: sc-7011, anti-β-actin: sc-47778- Santa Cruz Biotechnology, CA, USA), washed three times with TBS-T and then exposed to the appropriate HRP-conjugated secondary antibody for 1 h at room temperature. Membranes were again washed three times with TBS-T and immunoreactive bands were detected by enhanced chemiluminescence (ECL; GE Healthcare Bio-Sciences, Bs.As., Argentina) using standard X-ray film (Kodak X-OMAT AR; GE Healthcare Bio-Sciences). Immunoreactive bands were quantified using Image J[24].

2.2.9. Acyl-CoA (ACS) synthetase activity assay

The ACS activity was measured in cellular homogenates (6 x 10^6 cells) as described by Perez-Chacon *et al.* 2010 [29]. Briefly, 150 µl of cell lysates were incubated with buffer containing 20 mM $MgCl_2$, 10 mM ATP, 1 mM CoA, 1 mM 2-mercaptoethanol, 100 mM Tris-HCl (pH 8.0), and [^{3}H]-OA (0.2 µCi, 50 µM) at 37°C for 10 min. The reaction was stopped by addition of 2.25 ml isopropanol:heptane:1 M H_2SO_4 (40:10:1 v/v/v). After the addition of 1.5 ml heptane and 1 ml water, the mixture was centrifuged at 1000 x *g* for 5 min. The aqueous phase was then washed twice with 2 ml heptane containing 4 mg/ml OA, and finally the radioactivity was measured by liquid scintillation counting. ACS activity is expressed as dpm of [^{3}H]-oleoyl-CoA per µg of protein.

2.2.10. β-oxidation assay

β-oxidation was measured by means of the release of [^{3}H]-H_2O according to Moon and Rhead [30]. Confluent 24-well microplates were incubated at 37 °C for 4 h with serum-free RPMI containing: [^{3}H]-OA (0.5 μCi/well), OA (1.5 μM) and lipid-free BSA (4 mol OA/mol BSA) to allow [^{3}H]-OA incorporation. After incubation, the reaction mixture was removed and added to a centrifuge tube with 0.2 ml of 10% trichloroacetic acid. The mixture was centrifuged at 8500 x *g* for 5 min. Supernatants were removed and extracted with 1 ml isopropanol:heptane:1 M H_2SO_4 (40:10:1 v/v/v). The resultant aqueous phase was treated with 0.07 ml of 6 N NaOH and subjected to a Dowex- 1X8 column in a Pasteur pipette. The column was eluted with 5 ml of distilled water, and each eluate was collected in a scintillation vial for counting. Radioactivity corresponding to [^{3}H]-H_2O was determined in a liquid scintillation spectrometer.

2.2.11. TAG lipase activity assay

Cellular homogenates (6 x 10^6 cells, 100 μl) were incubated with [^{3}H]-Glycerol-TAG (350000 dpm/μmol) in 20 mM phosphate buffer, pH 7.0, at 37 °C for 30 min [31]. The reaction was stopped by addition of 5 ml chloroform:methanol (2:1 v/v). After the addition of 1 ml 0.05% $CaCl_2$, samples were centrifuged at 1000 x *g* for 5 min. Aqueous phases containing [^{3}H]-glycerol were collected in scintillation vials for counting. Organic phases were spotted onto TLC plates, overlaid with a monoacylglycerol (MAG) diacylglycerol (DAG) and TAG standards for separation of [^{3}H]-glycerol MAG, [^{3}H]-glycerol DAG and [^{3}H]-glycerol TAG. After iodine staining, spots were scraped into scintillation vials and quantified by liquid scintillation spectrometry. Results are normalized with protein content.

2.2.12. Thioflavin S staining

After incubation with secondary antibody, cells were stained with freshly prepared 0.05% Thioflavin S in ethanol: water 1:1 (v/v) for 5 min. They were then washed with 80% ethanol for 5 min and nuclei were stained with Hoechst. After washing with PBS, coverslips were mounted for fluorescence microscopy [32].

2.2.13. Determination of cell oxidant levels

Cell OS was evaluated using the probe 5 (or 6)-carboxy-2'7'-dichlorodihydrofluorescein diacetate (DCDCDHF) which can cross the membrane and following oxidation is converted into a fluorescent compound. After the corresponding treatments, the medium was discarded and RPMI medium containing 10 μM DCDCDHF was added. After 30 min of incubation at 37°C, the medium was removed; cells were rinsed three times with PBS and lysed in a buffer containing PBS and 1% NP-40. Fluorescence in the lysates (λex=495, λem=530) was measured in an SLM model 4800 fluorimeter (SLM Instruments, Urbana, IL) [24]. Results are expressed as AU of absorbance per μg of protein [AU/μg protein].

2.2.14. Determination of lipid peroxidation

Lipid peroxidation was determined by the thiobarbituric acid reactive substances (TBARS) assay, which involves derivatization of malondialdehyde with TBA to produce a pink product that is quantified in a UV-VIS spectrophotometer. Briefly, after treatments, cells were scraped off into 300 μl of ice-cold water and mixed with 0.5 ml of 30 % trichloroacetic acid. Then, 50 μl of 5 N HCl and 0.5 ml of 0.75 % TBA were added. Tubes were capped, the mixtures were heated at 100 °C for 30 min in a boiling water bath and the samples were centrifuged at 1000 x g for 10 min. TBARS were measured spectrophotometrically in the supernatant at 532 nm [24]. Results are expressed as a percentage of the control.

2.2.15. Measurement of LDH leakage

Lactate dehydrogenase (LDH) leakage was determined as previously described [24]. After treatments, incubation medium was centrifuged at 1000 x g for 10 min at 4 °C. The resulting supernatant was used to determine LDH activity, which was measured spectrophotometrically using an LDH-P UV AA kit, following the manufacturer's instructions. Briefly, the conversion rate of reduced nicotinamide adenine dinucleotide to oxidized nicotinamide adenine dinucleotide was followed at 340 nm. Results are expressed as a percentage of the control.

2.2.16. FA analysis

FA of all lipid classes from N27 cells (pcDNA and A53T α-syn) were quantified by gas chromatography (GC) after the addition of an internal standard (21:0) and conversion of the extracted dried lipids into methyl ester derivatives. After lipid extraction by the Bligh & Dyer method, fatty acid methyl esters (FAME) were prepared following the alternative method of the AOCS Ce 2-66 normative from the American Oil Chemists' Society, by transesterification with 2N KOH in anhydrous methanol. Separation and identification of the FAME were carried out in an Agilent 7820A gas chromatograph equipped with a split/splitless injector, a flame-ionization detector and a 30 m SP-2380 capillary column of 0.25 mm i.d. and 0.2 μm film thickness (Supelco Inc., Bellefonte, PA). The operating conditions were as follows: oven temperature, 170°C (15 min)–4 °C/min–210°C (10 min); injector and detector temperatures were set at 200ºC; injection volume, 2 μl; and carrier gas, hydrogen at 18,4 cm s−1. EZChrom Elite software (Agilent Technologies, Inc. 2006) was used for data analysis. FAME identification was carried out by comparison with the

certified standard Supelco FAME 10 mix 37 (CRM47885, Bellefonte, PA, USA), according to the official AOCS method Ce 1b-89.

2.2.17. Statistical analysis

Data represent the mean value ± SD of at least three independent experiments; each experiment was performed in triplicate. Statistical significance was determined by either Student's t-test or one-way ANOVA followed by a Tukey's test. p-values lower than 0.05 were considered statistically significant. For cytochemistry studies, 10 fields per sample were analyzed in each case. The Western blots shown are representative images of samples from three independent experiments.

3. Results

3.1. Characterization of lipid status in A53T α-syn neurons

We have previously reported that Fe exposure modulates neuronal lipid metabolism and that TAG content increases in response to oxidative injury [24]. In this work, our aim was to study the lipid metabolism status in neurons overexpressing A53T α-syn and exposed to Fe injury. For this purpose, we worked with dopaminergic N27 neurons (untransfected-UT) and two derived cell lines that stably express either the empty vector (pcDNA) or the mutant form of α-syn A53T (A53T α-syn). The expression of α-syn in A53T α-syn cells was evaluated by immunocytochemistry. A53T α-syn cells showed increased levels of the protein with respect to controls pcDNA and UT cells (Fig. 1A).

To evaluate whether A53T α-syn has any effect on lipid status we first checked TAG, PL and chol content. To determine whether the transfection and antibiotic-directed selection of

stable cell lines could affect lipid content, we also checked lipid levels in UT and pcDNA cells. Both UT and pcDNA cells showed similar chol, PL and TAG content (Fig. 1B-D). A53T α-syn cells displayed a 40 % increase in TAG levels with no changes in PL and chol content when compared with pcDNA and UT controls (Fig. 1B-D). Cell viability in A53T α-syn cells showed a slight decrease (10 %) with respect to controls (Fig. 1E). We also evaluated TAG content in two different neuronal lines (N27 and human IMR-32 cells) stably transfected with the wild type form of α-syn: while N27 cells showed no changes, levels of lipids were increased in IMR-32 cells (data not shown). We assume that levels of α-syn expression depending on the cellular type govern this lipid switch more than the specific form of the protein (mutated vs wild type). Our results demonstrate that α-syn overexpression in A53T α-syn cells is able to alter neuronal TAG content without substantial changes in cell viability. For this reason, our experimental system could constitute a cellular model for studying the early events of PD when the mutated A53T form of α-syn is present.

To confirm the increase in α-syn expression in A53T α-syn cells, protein levels were evaluated by Western blot. Cells transfected with the vector containing the A53T α-syn form displayed a 300 % increase in α-syn protein levels with respect to empty vector controls (Fig. 2A). In order to further characterize the TAG increase in A53T α-syn cells, we evaluated the presence of lipid droplets using Oil Red O staining. We observed an increase in lipid droplets formation in cells overexpressing the A53T form of α-syn compared to pcDNA controls (Fig. 2B). We also checked the dopaminergic marker Tyrosine Hydroxylase (TH) and detected no changes induced by A53T α-syn overexpression (Fig. 2C). The lack of TH alteration and the small changes observed in cell

viability (Fig. 1E) argue in favor of a mild injury produced by A53T α-syn overexpression that is accompanied by the accumulation of TAG, a rather unusual occurrence in healthy neurons.

Cumulative evidence indicates that α-syn overexpression and aggregation are associated with the presence of several changes in lipid metabolism [15,16,33–36]. To correlate the increase in TAG content observed in A53T α-syn cells with the above mentioned findings, we then checked acylation capacity by analyzing Acyl-CoA synthetase (ACS) activity. A53T α-syn cells displayed increased ACS specific activity, thus showing a higher FA availability (Fig. 3A). This higher FA bioavailability is a necessary condition for the increase in TAG levels; however another metabolic pathway requiring CoA esterification is mitochondrial FA β-oxidation, which we then proceeded to analyze by measuring [^{3}H]-H_2O release from [^{3}H]-OA pre-labeled cells. We detected no changes in FA β-oxidation when comparing pcDNA and A53T α-syn cells (Fig. 3B). Taking into account the higher ACS activity with no changes in FA β-oxidation levels observed in A53T α-syn cells and the increased TAG levels, the most probable fate of FA-CoA derivatives is their esterification in glycerol moieties. To discard the possibility that the TAG increase could be due to a downregulation of lipase activity, we also evaluated TAG hydrolysis in cellular lysates. For this purpose, we measured the generation of [^{3}H]-glycerol, [^{3}H]-glycerol MAG and [^{3}H]-glycerol DAG, using [^{3}H]-glycerol-TAG as substrate. We did not detect differences in the rate of TAG hydrolysis between pcDNA and A53T α-syn cells (Fig. 3C).

We also observed that A53T α-syn cells expressed higher levels (a 300% increase) of FAS than pcDNA cells (Fig. 3D). To evaluate the FA bioavailability, we then analyzed the total FA content in both cellular lines. We observed a 15 % increase in FA content in A53T α-

syn cells (Fig. 3E). Our results indicate that the overexpression of α-syn in A53T α-syn cells upregulates neuronal lipid metabolism by promoting an increase in neuronal TAG content.

3.2. Role of lipid metabolism in A53T α-syn cells

Based on the results demonstrating an increase in TAG levels in A53T α-syn cells, and to further investigate the far-reaching implications of α-syn overexpression for lipid metabolism we proceeded to investigate the effect of inhibiting FA and TAG *de novo* synthesis on the neuronal fate. For this purpose, we measured cell viability after pharmacological inhibition of key enzymes involved in both processes. A53T α-syn cells were more resistant to different concentrations of the pharmacological FAS inhibitor, Cerulenin (Fig. 4A). We also analyzed cellular viability in the presence of Malonyl-CoA, an allosteric inhibitor of the key enzyme in FA β-oxidation carnitine palmitoyl-transferase-1. We detected no alterations in cellular viability in pcDNA or A53T α-syn cells (Fig. 4B).

To evaluate the role of TAG *de novo* synthesis in the neuronal response to α-syn overexpression we used Triacsin C for inhibiting ACS, the enzyme responsible for FA activation before esterification in the glycerol backbone. A53T α-syn cells showed diminished viability in the presence of Triacsin C (Fig. 4C). In addition, we also used DL-Propranolol for inhibiting lipin-1, the rate-limiting step enzyme in TAG synthesis. The presence of DL-Propranolol rendered A53T α-syn cells more sensitive and affected cell viability (Fig. 4D), thus demonstrating that α-syn overexpression in A53T α-syn neurons increase TAG levels as a neuroprotective strategy. We cannot rule out that TAG appearance, rather unusual for a neuronal phenotype, could constitute an early marker of neuronal injury.

3.3. Effect of Fe exposure on A53T α-syn neurons

As previously stated, Fe accumulation and the consequent OS increase are hallmarks of the dopaminergic neuron environment in PD [18]. To evaluate the effect of the metal injury on A53T α-syn neurons, cells were exposed to Fe (1 mM) and α-syn aggregation and OS parameters were evaluated.

A53T α-syn cells exposed to Fe showed increased levels of α-syn compared with cells treated with vehicle (Fig. 5). A similar effect was observed in pcDNA cells. This is in agreement with previous findings that the metal is able to modulate α-syn expression at the translational level [37]. To determine the effect of Fe on A53T α-syn aggregation we used the intracellular probe Thioflavin S. The extent of Thioflavin S fluorescence indicates the presence of protein aggregates. A53T α-syn cells exposed to Fe showed the highest levels of fluorescence, thus demonstrating that metal exposure induced increased α-syn aggregation (Fig. 5).

To determine the role of Fe in neuronal injury in A53T α-syn cells, OS markers were then evaluated. The reactive oxygen species (ROS) content (measured by using the probe DCDCDHF) observed in pcDNA cells exposed to Fe was higher than that in A53T α-syn cells (Fig. 6A). Moreover, ROS levels were reduced by α-syn overexpression in A53T α-syn cells after Fe challenge. In harmony with these results, Fe-exposed A53T α-syn cells showed a decrease in lipid peroxide levels and LDH release compared with pcDNA cells (Fig. 6B and C). However, A53T α-syn cells exposed to Fe showed the highest levels of TAG (Fig. 6D). These findings suggest that the stable expression of α-syn in A53T α-syn cells could exert a protective function against Fe-induced OS in dopaminergic neurons.

This effect could be mediated at least in part by the sequestration of Fe during the aggregation of A53T α-syn.

4. Discussion

One of the most characteristic events in PD is the accumulation and aggregation of different α-syn variants in the *substancia nigra* pars compacta. The mutated form of the presynaptic protein α-syn, A53T, is one of the leading causes of early-onset familial PD. Besides overexpression and aggregation of different α-syn variants, another intriguing characteristic of PD is Fe accumulation [38,39]. The role of Fe in the ethiopathogenesis of this pathology is supported not only by its higher levels in the brain (*post-mortem* determination in PD patients) but also by reports showing that the administration of Fe chelators and the overexpression of Fe-binding proteins are neuroprotective strategies in PD animal models [23,40,41]. In line with this, the A53T α-syn mutant presents high Fe affinity and an increased rate of oligomerization when complexed with the metal [9,22]. Recent *in vivo* experiments in *Drosophila*, showed that Fe overload can trigger different neurodegeneration phenotypes in the presence of the A53T α-syn mutant, clear evidence of the interaction between the mutated protein and the metal [42].

Our studies reveal that A53T α-syn neurons exposed to Fe displayed lower ROS and lipid peroxidation levels than pcDNA cells. The decreased in OS markers in the presence of A53T α-syn cells might be a consequence of the enhanced Fe binding properties of the mutated form of α-syn [9,22]. It is important to note that our experiments were performed with Fe 1 mM, a concentration we have previously shown to trigger mild oxidative injury in dopaminergic neurons [24]. Under our experimental conditions an increase in the

aggregated form of α-syn (measured as Thioflavin S fluorescence) can be observed in Fe-exposed neurons. It has been reported that higher metal concentrations (10 mM) promote protein fibrillation [9]. Another consequence of the Fe binding capacity of A53T α-syn might be its enhanced aggregation. This metal -induced aggregation could be implicated in the metal scavenger activity of the mutated protein, thus diminishing Fe oxidant activity. In this connection, wild-type α-syn has been reported as a ferrireductase, which may help cells to maintain the Fe(II)/Fe(III) ratio necessary for dopamine synthesis [19]. The possibility cannot be discarded that the mutant A53T-α-syn -either because of the substitution of alanine by threonine, or because of the aggregation induced by the metal- is unable to act as a ferrireductase, thus lowering the Fe (II) levels necessary for the Fenton reaction. Protein concentration may be another factor involved. In experiments performed with hydroxyurea in *Saccharomyces cerevisiae*, the balance between protection and toxicity was dependent on the α-syn concentration and its subcellular localization [43]. Moreover, it cannot be ruled out that the apparent protective role of A53T α-syn observed in our experiments is due to an early function that when lost, triggers neurodegeneration.

Equally striking is the fact that α-syn has a strong tendency to bind FA, PL and lipid droplets and to alter several aspects of lipid metabolism [15,44–46]. Moreover HEK 293 cells overexpressing A53T α-syn and subjected to FA overload showed increased TAG levels [13,45]. Based on these data, it can be hypothesized that there is a strong correlation between neuronal lipid metabolism, α-syn pathology and Fe accumulation in PD. In harmony with this hypothesis, we show here that the stable expression of A53T α-syn in dopaminergic neurons disturbs neuronal lipid metabolism and that this effect is even more pronounced in the presence of Fe. An unexpected characteristic of A53T α-syn neurons is

the higher TAG content and increased lipid droplet formation with respect to control cells. The rise in TAG levels was accompanied by an increase in ACS activity without alterations in FA β-oxidation or TAG hydrolysis. Our results demonstrate that TAG accumulation was enhanced mainly by the increased bioavailability of FA-CoA derivatives. Since PL content was not affected, the unique consequence of this exacerbated ACS activity was the elevated levels of TAG. Based on our experiments performed with the mutant A53T we cannot rule out that others forms of α-syn overexpression had the same effect depending on the levels of protein expression. Pioneering work from Murphy's lab demonstrated that wild-type α-syn, but not mutants, modulate brain arachidonate metabolism through the modulation of ACS activity [47]. Further studies demonstrate that the ablation of α-syn expression (SNCA knock-out mice) induces a significant reduction in the incorporation rate of arachidonic and docosahexaenoic acid into brain PL, thus promoting increased proinflammatory cytokine secretion [10,11,36]. Moreover, it has been reported that α-syn mutants (A53T and A30P) displayed differential TAG turnover in lipid loaded HeLa cells [45].

Our results demonstrate that α-syn overexpression in A53T α-syn cells induces a TAG increase that could be a consequence of ACS upregulation, revealing its involvement in lipid metabolism. This unexpected lipid metabolic switch for a neuronal cell could indicate the onset of the neurodegenerative process.

5. Conclusions

We have previously shown that during Fe-induced OS, the increase in TAG content in dopaminergic neurons is a smart neuroprotective approach for preserving arachidonic acid from lipid peroxidation [24]. In agreement with this, A53T α-syn cells were also able to

modulate TAG metabolism to face mild oxidative damage. Our results suggest that the early cellular events triggered by α-syn in A53T cells involve alterations in lipid metabolism that lead to TAG accumulation and neuroprotection against Fe-induced oxidative stress. This metabolic switch could be indicative of the early onset of dopaminergic neurodegeneration (Graphical Abstract).

6. Acknowledgements

SSC was a PhD fellow of the Consejo Nacional de Investigaciones Científicas y Técnicas (CONICET). GAS and NA are research members of CONICET. This work was supported by grants from the Agencia Nacional de Promoción Científica y Tecnológica www.agencia.mincyt.gob.ar/ (PICT2010-0936, PICT2013-0987), CONICET www.conicet.gov.ar (PIP1122009010068) and the Universidad Nacional del Sur www.uns.edu.ar (PGI24B226) to GAS.

Authors wish to thank Wiener laboratories for kindly providing LDH kits and Dr. Benjamin Wolozin for kindly providing the A53T α-syn DNA construct. Authors are also grateful to Ignacio Bergé and Dr. Ana Maria Roccamo for assistance in molecular biology techniques, and Dr. Ana Ves Losada for kindly providing Triacsin C.

Figure legends

Fig. 1. Lipid status in A53T α-syn-N27 cells (A) α-syn expression in dopaminergic neurons. Fluorescence photomicrographs of UT, pcDNA and A53T α-syn cells. Representative images from three different experiments are shown. Fluorescence intensity

quantification (AU) is shown in the graph below the images. (B) Chol levels in UT, pcDNA and A53T α-syn neurons. Chol levels were determined by a colorimetric assay as described in Materials and Methods. (C) Lipid phosphorus content in UT, pcDNA and A53T α-syn cells. Total lipid phosphorus content was determined by the method of Rouser et al. (Rouser et al., 1970). Results are expressed as μg of lipid phosphorus. (D) TAG content in UT, pcDNA and A53T α-syn cells. TAG content was determined by an enzyme-specific colorimetric assay as specified in Materials and Methods. (E) Determination of cellular viability in UT, pcDNA and A53T α-syn cells using MTT reduction assay. (B, D-E) Results are expressed as a percentage of the control and represent mean ± SD (n=3). *$p < 0.05$ with respect to the control condition.

Fig. 2. Characterization of A53T α-syn cells. (A) Immunoblot of α-syn expression levels in lysates from pcDNA and A53T α-syn cells from two independent experiments. One representative blot of three different experiments is presented. Bands of α-syn (19 kDa) were quantified through scanning densitometry. The data in the graph on the right represent the ratio between α-syn and β-actin (mean ± SD of three different experiments, *$p < 0.05$ with respect to the control). (B) Oil Red O staining for lipid droplets. Fluorescence photomicrographs show the formation of lipid droplets (white arrows) in pcDNA and A53T α-syn cells. (C) Expression of TH in pcDNA and A53T α-syn neurons. Pictures show TH expression levels analyzed by immunocytochemistry. The graph below represents the fluorescence intensity (AU). (B-C) DAPI was used for nuclear staining.

Fig. 3. Characterization of lipid metabolism in A53T α-syn cells. (A) ACS activity in pcDNA and A53T α-syn cells was determined through the radioactivity assay described in Materials and Methods. Results are expressed as dpm of [^{3}H] oleoyl-CoA per μg of protein

and represent mean ± SD (n=3). *p < 0.05 with respect to the control condition. (B) FA β-oxidation was measured in pcDNA and A53T α-syn neurons by means of the release of [^{3}H]-H_2O as described in Materials and Methods. Results are expressed as dpm of [^{3}H]-H_2O per ml and represent mean ± SD (n=3, ns= no significant difference with respect to the control condition). (C) TAG lipase activity was studied in pcDNA and A53T α-syn neurons as described in Materials and Methods. Data represent dpm of tritiated species (glycerol, MAG and DAG) normalized with protein content. Results represent mean ± SD (n=3, ns= no significant difference with respect to the control condition). (D) Expression levels of FAS in pcDNA and A53T α-syn neurons were analyzed by Western blot. Western blot images are representative of three different experiments. (E) Total FA content. FA of all lipid classes from pcDNA and A53T α-syn cells were quantified by GC as describe in Materials and Methods. Results are expressed as μg FA normalized by phospholipid P content and represent mean ± SD (n=3, * p < 0.05 with respect to the control condition).

Fig. 4. Role of lipid metabolism enzymes in A53T α-syn cell viability. The schematic view shows the FA synthesis/degradation and Kennedy pathways and site of action of the pharmacological inhibitors: Cerulenin (FAS inhibitor), Malonyl-CoA (β-oxidation inhibitor), Triacsin C (ACS inhibitor) and DL-Propranolol (lipin 1 inhibitor). (A) Effect of the FAS inhibitor Cerulenin on cell viability. pcDNA and A53T α-syn cells were exposed to different concentrations of Cerulenin or its vehicle and cell viability was assayed by MTT reduction. (B) Effect of the β-oxidation inhibitor Malonyl-CoA on cell viability. pcDNA and A53T α-syn cells were treated with different concentrations of Malonyl-CoA or its vehicle and cell viability was assayed by MTT reduction. (C) Effect of Triacsin C on cell viability. pcDNA and A53T α-syn cells were exposed to the ACS inhibitor Triacsin C

(5 μM) or its vehicle and cell viability was evaluated by the MTT reduction assay. (D) Effect of DL-Propranolol on cell viability. pcDNA and A53T α-syn cells were treated with the lipin inhibitor DL-Propranolol (100 μM) or its vehicle and cell viability was determined by the MTT reduction assay. (A-D) Results are expressed as a percentage of the control and represent mean ± SD (n=3, * $p< 0.05$ with respect to the control condition).

Fig. 5. A53T α-syn aggregation after Fe exposure. pcDNA and A53T α-syn neurons cells were treated under control conditions and in the presence of Fe (1 mM) for 24 h. After treatments, cells were processed for immunocytochemistry studies with an antibody against α-syn (red) and subsequently incubated with Thioflavin S (green) as described in Materials and Methods. Nuclei were stained with Hoechst (blue). Representative images of three different experiments are shown. The data in the graphs represent the fluorescence intensity of α-syn (left panel) and Thioflavin S (right panel) (mean ± SD of three different experiments, * $p < 0.05$ with respect to the control).

Fig. 6. Effect of Fe exposure on the neuronal response to A53T α-syn variant. (A) Cell oxidant levels in pcDNA and A53T α-syn cells after Fe exposure. Cells were treated with Fe (1 mM) or its vehicle for 24 h and subsequently incubated in the presence of 10 μM DCDCDHF in order to determine ROS levels. Results are expressed as AU normalized by protein content and represent mean ± SD (n=3, * $p< 0.05$ with respect to the control condition). (B) Lipid peroxide levels in pcDNA and A53T α-syn cells exposed to Fe. Cells were treated as described in A and lipid peroxidation was evaluated by TBARS determination. Results are expressed as a percentage of the control and represent mean ± SD (n=10, * $p < 0.05$ with respect to the control condition). (C) Plasma membrane permeability in pcDNA and A53T α-syn cells after Fe exposure. LDH leakage assay was

assessed after cells were treated with the conditions described in A. Results are expressed as a percentage of the control and represent mean ± SD (n=6, * $p < 0.05$ with respect to the control condition). (D) Effect of Fe treatment on TAG levels in A53T α-syn cells. TAG content was analyzed in pcDNA and A53T α-syn cells treated as described in A. Results are expressed as a percentage of the control and represent mean ± SD (n=3, * $p < 0.05$ with respect to the control condition).

Graphical Abstract. Effect of A53T α-syn overexpression and Fe exposure on neuronal lipid metabolism. A53T α-syn overexpression increased FAS expression levels, ACS activity and TAG content. A53T α-syn diminished ROS generation and lipid peroxidation induced by Fe-exposure. A53T α-syn cells exposed to Fe showed increased TAG content. The appearance of TAG in A53T α-syn cells could constitute a marker of neuronal injury during the early stages of PD.

References

[1] K.L. Lim, C.W. Zhang, Molecular events underlying Parkinson's disease - an interwoven tapestry, Front. Neurol. 4 APR (2013). doi:10.3389/fneur.2013.00033.

[2] S. Gallegos, C. Pacheco, C. Peters, C. Opazo, L.G. Aguayo, Features of alpha-synuclein that could explain the progression and irreversibility of Parkinson's disease, Front. Neurosci. 9 (2015). doi:10.3389/fnins.2015.00059.

[3] A. Hatami, M.F. Chesselet, Transgenic rodent models to study alpha-synuclein pathogenesis, with a focus on cognitive deficits, Curr. Top. Behav. Neurosci. 22 (2014) 303–330. doi:10.1007/7854_2014_355.

[4] A. Recasens, B. Dehay, Alpha-synuclein spreading in Parkinsonâ€™s disease, Front. Neuroanat. 8 (2014). doi:10.3389/fnana.2014.00159.

[5] B.I. Giasson, J.E. Duda, S.M. Quinn, B. Zhang, J.Q. Trojanowski, V.M.-Y. Lee, Neuronal alpha-synucleinopathy with severe movement disorder in mice expressing A53T human alpha-synuclein., Neuron. 34 (2002) 521–533. doi:10.1016/S0896-6273(02)00682-7.

[6] B.K. Harvey, Y. Wang, B.J. Hoffer, Transgenic rodent models of Parkinson's disease., Acta Neurochir. Suppl. 101 (2008) 89–92. doi:10.1007/978-3-211-78205-7.

[7] S. Gispert, N. Brehm, J. Weil, K. Seidel, U. Rï¿½b, B. Kern, M. Walter, J. Roeper, G. Auburger, Potentiation of neurotoxicity in double-mutant mice with Pink1 ablation and A53T-SNCA overexpression, Hum. Mol. Genet. 24 (2015) 1061–1076. doi:10.1093/hmg/ddu520.

[8] K. Markopoulou, D.W. Dickson, R.D. McComb, Z.K. Wszolek, L. Katechalidou, L. Avery, M.S. Stansbury, B.A. Chase, Clinical, neuropathological and genotypic variability in SNCA A53T familial Parkinson's disease, Acta Neuropathol. 116 (2008) 25–35. doi:10.1007/s00401-008-0372-4.

[9] N. Ostrerova-Golts, L. Petrucelli, J. Hardy, J.M. Lee, M. Farer, B. Wolozin, The A53T alpha-synuclein mutation increases iron-dependent aggregation and toxicity., J. Neurosci. 20 (2000) 6048–6054. doi:20/16/6048 [pii].

[10] M.Y. Golovko, T.A. Rosenberger, S. Feddersen, N.J. Færgeman, E.J. Murphy, α-Synuclein gene ablation increases docosahexaenoic acid incorporation and turnover in brain phospholipids, J. Neurochem. 101 (2007) 201–211. doi:10.1111/j.1471-

4159.2006.04357.x.

[11] M.Y. Golovko, G. Barceló-Coblijn, P.I. Castagnet, S. Austin, C.K. Combs, E.J. Murphy, The role of α-synuclein in brain lipid metabolism: A downstream impact on brain inflammatory response, in: Mol. Cell. Biochem., 2009: pp. 55–66. doi:10.1007/s11010-008-0008-y.

[12] I. Rappley, D.S. Myers, S.B. Milne, P.T. Ivanova, M.J. Lavoie, H.A. Brown, D.J. Selkoe, Lipidomic profiling in mouse brain reveals differences between ages and genders, with smaller changes associated with ??-synuclein genotype, J. Neurochem. 111 (2009) 15–25. doi:10.1111/j.1471-4159.2009.06290.x.

[13] R. Sharon, I. Bar-Joseph, M.P. Frosch, D.M. Walsh, J.A. Hamilton, D.J. Selkoe, The formation of highly soluble oligomers of alpha-synuclein is regulated by fatty acids and enhanced in Parkinson's disease., Neuron. 37 (2003) 583–95. doi:S0896627303000242 [pii].

[14] R.J. Perrin, W.S. Woods, D.F. Clayton, J.M. George, Exposure to Long Chain Polyunsaturated Fatty Acids Triggers Rapid Multimerization of Synucleins, J. Biol. Chem. 276 (2001) 41958–41962. doi:10.1074/jbc.M105022200.

[15] V. Ruipérez, F. Darios, B. Davletov, Alpha-synuclein, lipids and Parkinson's disease, Prog. Lipid Res. 49 (2010) 420–428. doi:10.1016/j.plipres.2010.05.004.

[16] R. Sharon, M.S. Goldberg, I. Bar-Josef, R. a Betensky, J. Shen, D.J. Selkoe, Alpha-Synuclein occurs in lipid-rich high molecular weight complexes, binds fatty acids, and shows homology to the fatty acid-binding proteins., Proc. Natl. Acad. Sci. U. S. A. 98 (2001) 9110–9115. doi:10.1073/pnas.171300598.

[17] R.M. Uranga, N.P. Alza, M.A. Conde, S.S. Antollini, G.A. Salvador, Phosphoinositides: Two-Path Signaling in Neuronal Response to Oligomeric Amyloid β Peptide, Mol. Neurobiol. 54 (2017) 3236–3252. doi:10.1007/s12035-016-9885-3.

[18] K.J. Barnham, A.I. Bush, Metals in Alzheimer's and Parkinson's Diseases, Curr. Opin. Chem. Biol. 12 (2008) 222–228. doi:10.1016/j.cbpa.2008.02.019.

[19] D.R. Brown, alpha-Synuclein as a ferrireductase., Biochem. Soc. Trans. 41 (2013) 1513–1517. doi:10.1042/BST20130130.

[20] P. Davies, D. Moualla, D.R. Brown, Alpha-synuclein is a cellular ferrireductase, PLoS One. 6 (2011). doi:10.1371/journal.pone.0015814.

[21] Bharathi, K.S.J. Rao, Molecular understanding of copper and iron interaction with alpha-synuclein by fluorescence analysis., J. Mol. Neurosci. 35 (2008) 273–81. doi:10.1007/s12031-008-9076-4.

[22] J.L. Billings, D.J. Hare, M. Nurjono, I. Volitakis, R.A. Cherny, A.I. Bush, P.A. Adlard, D.I. Finkelstein, Effects of Neonatal Iron Feeding and Chronic Clioquinol Administration on the Parkinsonian Human A53T Transgenic Mouse, ACS Chem. Neurosci. 7 (2016) 360–366. doi:10.1021/acschemneuro.5b00305.

[23] D.I. Finkelstein, D.J. Hare, J.L. Billings, A. Sedjahtera, M. Nurjono, E. Arthofer, S. George, J.G. Culvenor, A.I. Bush, P.A. Adlard, Clioquinol Improves Cognitive, Motor Function, and Microanatomy of the Alpha-Synuclein hA53T Transgenic Mice, ACS Chem. Neurosci. 7 (2016) 119–129. doi:10.1021/acschemneuro.5b00253.

[24] S.S. Campos, G.R. Diez, G.M. Oresti, G.A. Salvador, Dopaminergic neurons respond to iron-induced oxidative stress by modulating lipid acylation and deacylation cycles, PLoS One. 10 (2015). doi:10.1371/journal.pone.0130726.

[25] E.G. Bligh, W.J. Dyer, A RAPID METHOD OF TOTAL LIPID EXTRACTION AND PURIFICATION, Can. J. Biochem. Physiol. 37 (1959) 911–917. doi:10.1139/o59-099.

[26] G. Rouser, S. Fleischer, A. Yamamoto, Two dimensional thin layer chromatographic separation of polar lipids and determination of phospholipids by phosphorus analysis of spots, Lipids. 5 (1970) 494–496. doi:10.1007/BF02531316.

[27] J. Bi, Y. Xiang, H. Chen, Z. Liu, S. Gronke, R.P. Kuhnlein, X. Huang, Opposite and redundant roles of the two Drosophila perilipins in lipid mobilization, J. Cell Sci. 125 (2012) 3568–3577. doi:10.1242/jcs.101329.

[28] M.M. Bradford, A rapid and sensitive method for the quantitation of microgram quantities of protein using the principle of protein dye binding, Anal. Biochem. 72 (1976) 248–254. doi:10.1016/0003-2697(76)90527-3.

[29] G. Pérez-Chacón, A.M. Astudillo, V. Ruipérez, M. a Balboa, J. Balsinde, Signaling role for lysophosphatidylcholine acyltransferase 3 in receptor-regulated arachidonic acid reacylation reactions in human monocytes., J. Immunol. 184 (2010) 1071–1078. doi:10.4049/jimmunol.0902257.

[30] A. Moon, W.J. Rhead, Complementation analysis of fatty acid oxidation disorders., J. Clin. Invest. 79 (1987) 59–64. doi:10.1172/JCI112808.

[31] A.C. Pascual, V.L. Gaveglio, N.M. Giusto, S.J. Pasquaré, Aging modifies the

enzymatic activities involved in 2-arachidonoylglycerol metabolism, BioFactors. 39 (2013) 209–220. doi:10.1002/biof.1055.

[32] D.F. Lázaro, E.F. Rodrigues, R. Langohr, H. Shahpasandzadeh, T. Ribeiro, P. Guerreiro, E. Gerhardt, K. Kröhnert, J. Klucken, M.D. Pereira, B. Popova, N. Kruse, B. Mollenhauer, S.O. Rizzoli, G.H. Braus, K.M. Danzer, T.F. Outeiro, Systematic Comparison of the Effects of Alpha-synuclein Mutations on Its Oligomerization and Aggregation, PLoS Genet. 10 (2014). doi:10.1371/journal.pgen.1004741.

[33] C. Fecchio, G. De Franceschi, A. Relini, E. Greggio, M. Dalla Serra, L. Bubacco, P. Polverino De Laureto, α-synuclein oligomers induced by docosahexaenoic acid affect membrane integrity, PLoS One. 8 (2013). doi:10.1371/journal.pone.0082732.

[34] N. Shioda, Y. Yabuki, Y. Kobayashi, M. Onozato, Y. Owada, K. Fukunaga, FABP3 protein promotes α-synuclein oligomerization associated with 1-Methyl-1,2,3,6-tetrahydropiridine-induced neurotoxicity, J. Biol. Chem. 289 (2014) 18957–18965. doi:10.1074/jbc.M113.527341.

[35] E. Yakunin, V. Loeb, H. Kisos, Y. Biala, S. Yehuda, Y. Yaari, D.J. Selkoe, R. Sharon, α-Synuclein neuropathology is controlled by nuclear hormone receptors and enhanced by docosahexaenoic acid in a mouse model for Parkinson's disease, Brain Pathol. 22 (2012) 280–294. doi:10.1111/j.1750-3639.2011.00530.x.

[36] P.I. Castagnet, M.Y. Golovko, G.C. Barceló-Coblijn, R.L. Nussbaum, E.J. Murphy, Fatty acid incorporation is decreased in astrocytes cultured from α-synuclein gene-ablated mice, J. Neurochem. 94 (2005) 839–849. doi:10.1111/j.1471-4159.2005.03247.x.

[37] F. Febbraro, M. Giorgi, S. Caldarola, F. Loreni, M. Romero-Ramos, ??-Synuclein expression is modulated at the translational level by iron, Neuroreport. 23 (2012) 576–580. doi:10.1097/WNR.0b013e328354a1f0.

[38] D.W. Lee, J.K. Andersen, Iron elevations in the aging Parkinsonian brain: A consequence of impaired iron homeostasis?, J. Neurochem. 112 (2010) 332–339. doi:10.1111/j.1471-4159.2009.06470.x.

[39] F.A. Zucca, J. Segura-Aguilar, E. Ferrari, P. Muñoz, I. Paris, D. Sulzer, T. Sarna, L. Casella, L. Zecca, Interactions of iron, dopamine and neuromelanin pathways in brain aging and Parkinson's disease, Prog. Neurobiol. 155 (2017) 96–119. doi:10.1016/j.pneurobio.2015.09.012.

[40] A.A. Belaidi, A.I. Bush, Iron neurochemistry in Alzheimer's disease and Parkinson's disease: targets for therapeutics, J. Neurochem. (2016) 179–197. doi:10.1111/jnc.13425.

[41] L. Jin, J. Wang, L. Zhao, H. Jin, G. Fei, Y. Zhang, M. Zeng, C. Zhong, Decreased serum ceruloplasmin levels characteristically aggravate nigral iron deposition in Parkinson's disease, Brain. 134 (2011) 50–58. doi:10.1093/brain/awq319.

[42] Z.J. Zhu, K.C. Wu, W.H. Yung, Z.M. Qian, Y. Ke, Differential interaction between iron and mutant alpha-synuclein causes distinctive Parkinsonian phenotypes in Drosophila, Biochim. Biophys. Acta - Mol. Basis Dis. 1862 (2016) 518–525. doi:10.1016/j.bbadis.2016.01.002.

[43] X. Liu, Y.J. Lee, L.C. Liou, Q. Ren, Z. Zhang, S. Wang, S.N. Witt, Alpha-synuclein functions in the nucleus to protect against hydroxyurea-induced replication stress in

yeast, Hum. Mol. Genet. 20 (2011) 3401–3414. doi:10.1093/hmg/ddr246.

[44] K. Broersen, D. van den Brink, G. Fraser, M. Goedert, B. Davletov, Alpha-synuclein adopts an alpha-helical conformation in the presence of polyunsaturated fatty acids to hinder micelle formation., Biochemistry. 45 (2006) 15610–6. doi:10.1021/bi061743l.

[45] N.B. Colebc, D.D. Murphy, T. Grider, S. Rueter, D. Brasaemle, R.L. Nussbaum, Lipid droplet binding and oligomerization properties of the Parkinson's disease protein α-synuclein, J. Biol. Chem. 277 (2002) 6344–6352. doi:10.1074/jbc.M108414200.

[46] G. De Franceschi, E. Frare, M. Pivato, A. Relini, A. Penco, E. Greggio, L. Bubacco, A. Fontana, P.P. De Laureto, Structural and morphological characterization of aggregated species of α-synuclein induced by docosahexaenoic acid, J. Biol. Chem. 286 (2011) 22262–22274. doi:10.1074/jbc.M110.202937.

[47] M.Y. Golovko, T.A. Rosenberger, N.J. Faergeman, S. Feddersen, N.B. Cole, I. Pribill, J. Berger, R.L. Nussbaum, E.J. Murphy, Acyl-CoA synthetase activity links wild-type but not mutant alpha-synuclein to brain arachidonate metabolism., Biochemistry. 45 (2006) 6956–6966. doi:10.1021/bi0600289.

Figure 2

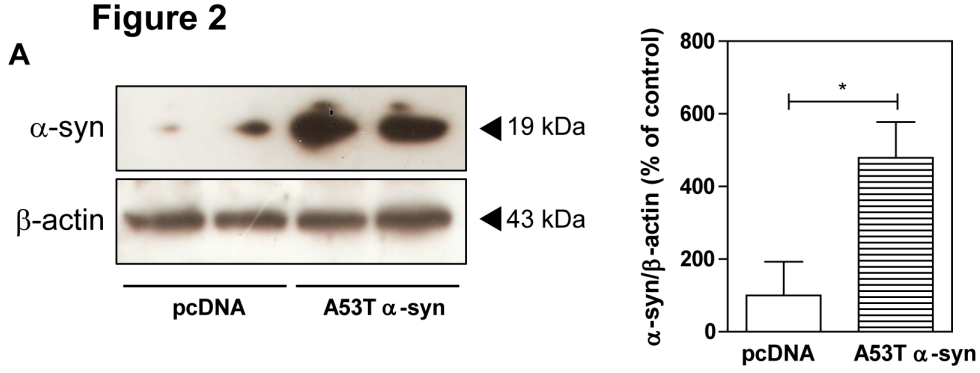
A
α-syn
β-actin
19 kDa
43 kDa
pcDNA
A53T α-syn
α-syn/β-actin (% of control)
800
600
400
200
0
*
pcDNA
A53T α-syn

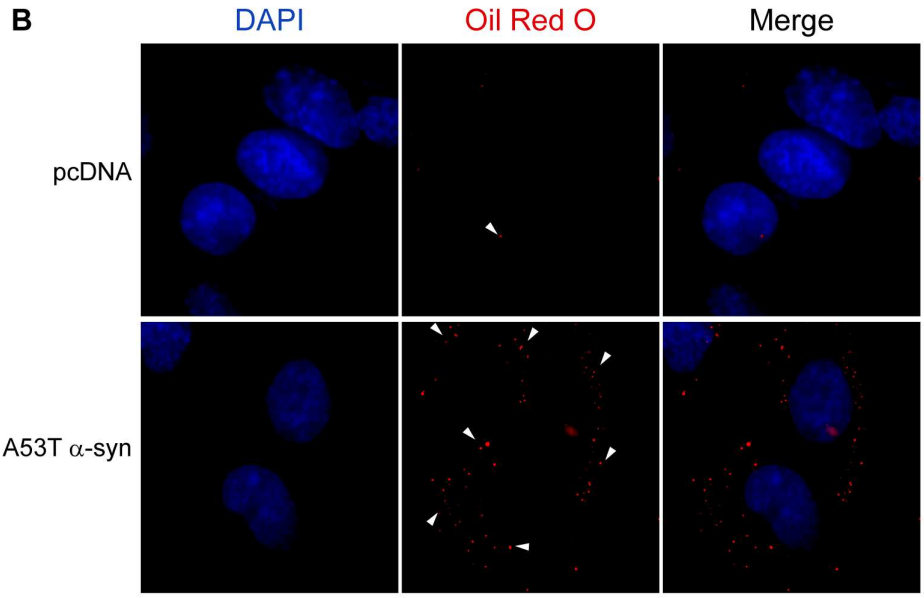
B
DAPI
Oil Red O
Merge
pcDNA
A53T α-syn

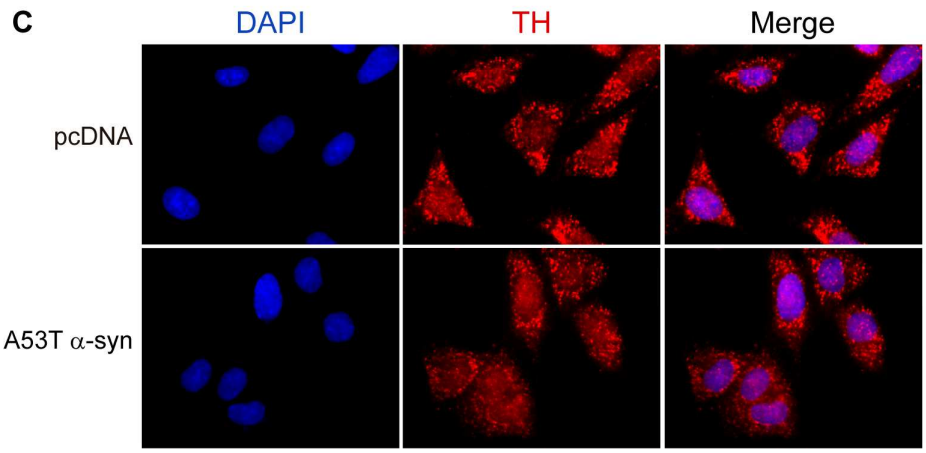
C
DAPI
TH
Merge
pcDNA
A53T α-syn

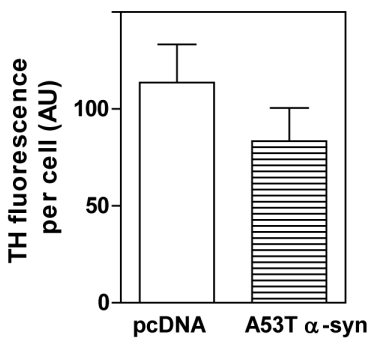
TH fluorescence per cell (AU)
100
50
0
pcDNA
A53T α-syn

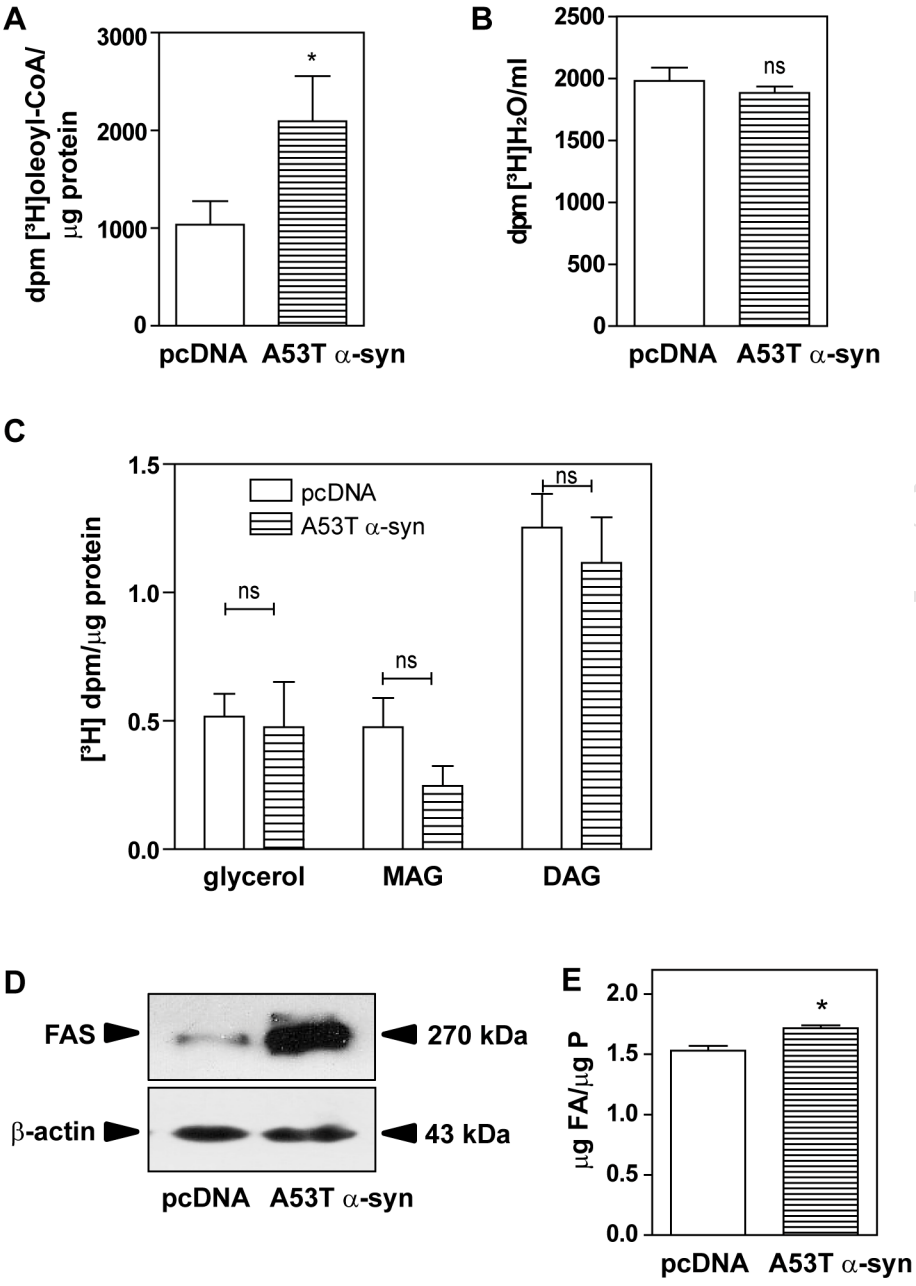
A
dpm [³H]oleoyl-CoA/ µg protein
3000
2000
1000
0
*
pcDNA
A53T α-syn
B
dpm [³H]H₂O/ml
2500
2000
1500
1000
500
0
ns
pcDNA
A53T α-syn
C
[³H] dpm/µg protein
1.5
1.0
0.5
0.0
pcDNA
A53T α-syn
ns
ns
ns
glycerol
MAG
DAG
D
FAS
270 kDa
β-actin
43 kDa
pcDNA
A53T α-syn
E
µg FA/µg P
2.0
1.5
1.0
0.5
0.0
*
pcDNA
A53T α-syn

Figure 3

Figure 4

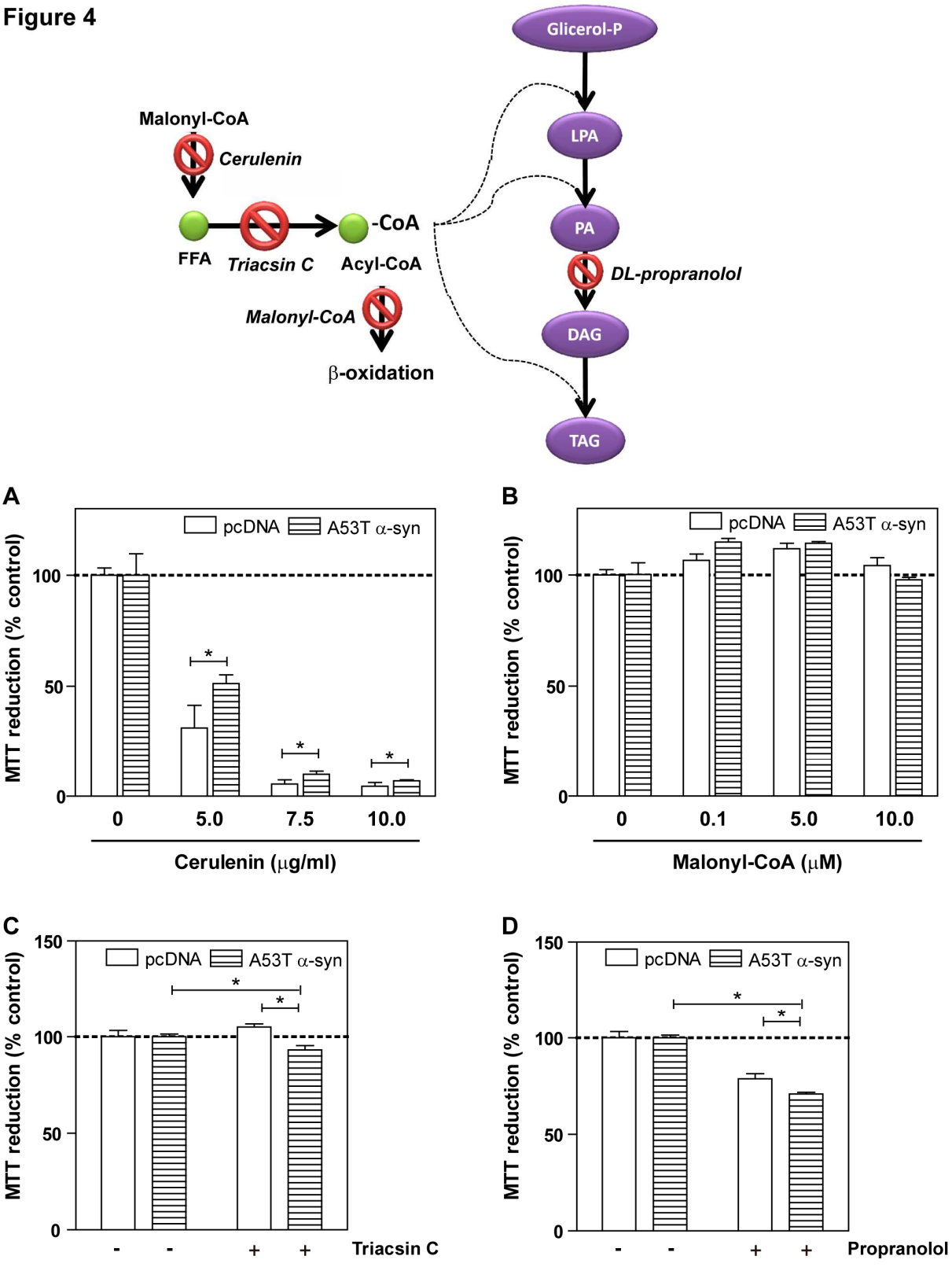
Glicerol-P
LPA
PA
DL-propranolol
DAG
TAG
Malonyl-CoA
Cerulenin
-CoA
FFA
Triacsin C
Acyl-CoA
Malonyl-CoA
β-oxidation
A
pcDNA
A53T α-syn
MTT reduction (% control)
100
50
0
0
5.0
7.5
10.0
Cerulenin (μg/ml)
B
pcDNA
A53T α-syn
MTT reduction (% control)
100
50
0
0
0.1
5.0
10.0
Malonyl-CoA (μM)
C
150
pcDNA
A53T α-syn
MTT reduction (% control)
100
50
0
- - + +
Triacsin C
D
150
pcDNA
A53T α-syn
MTT reduction (% control)
100
50
0
- - + +
Propranolol

Figure 5

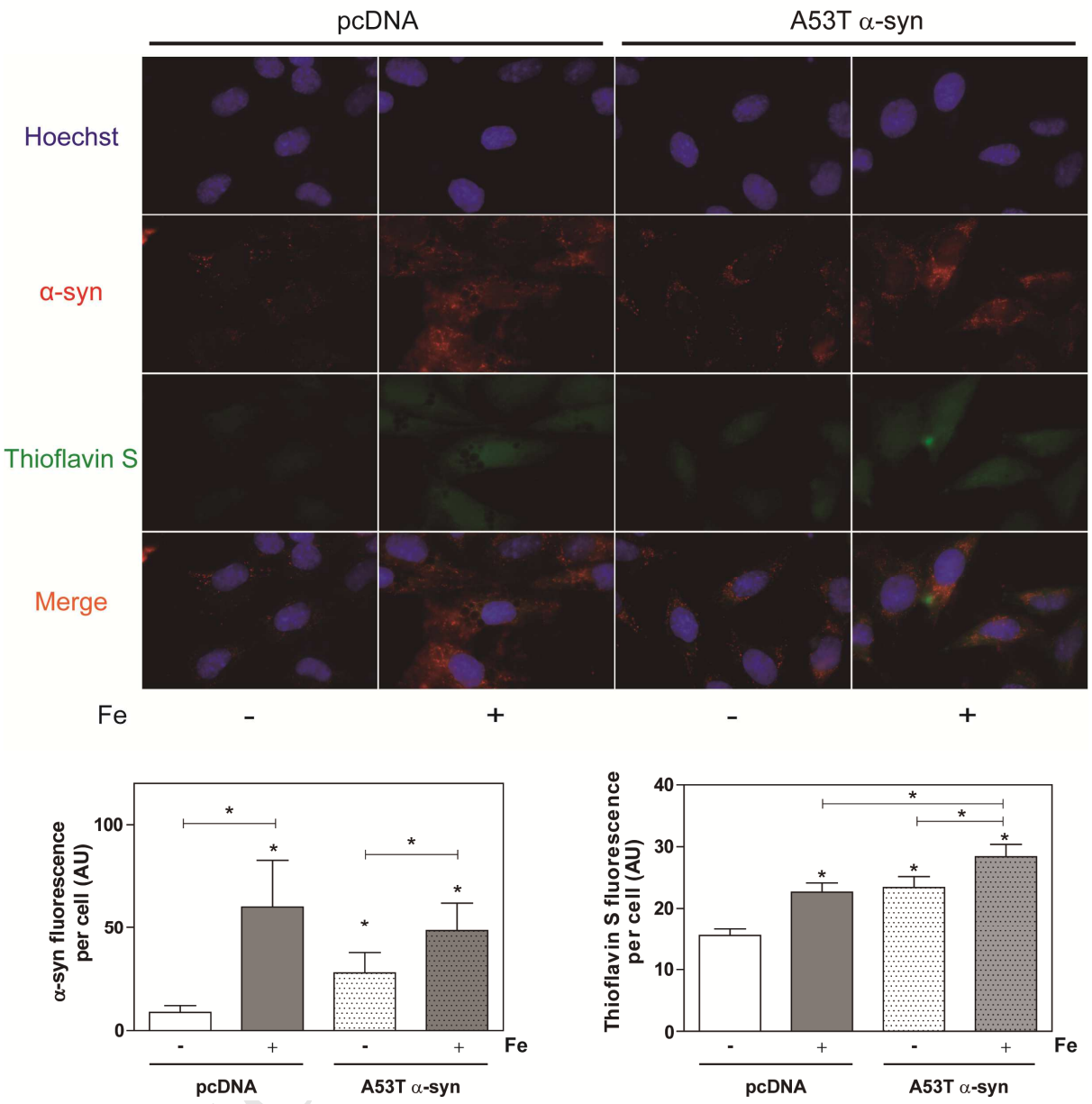
pcDNA
A53T α-syn
Hoechst
α-syn
Thioflavin S
Merge
Fe
-
+
-
+
α-syn fluorescence per cell (AU)
100
50
0
pcDNA
A53T α-syn
Thioflavin S fluorescence per cell (AU)
40
30
20
10
0

Figure 6

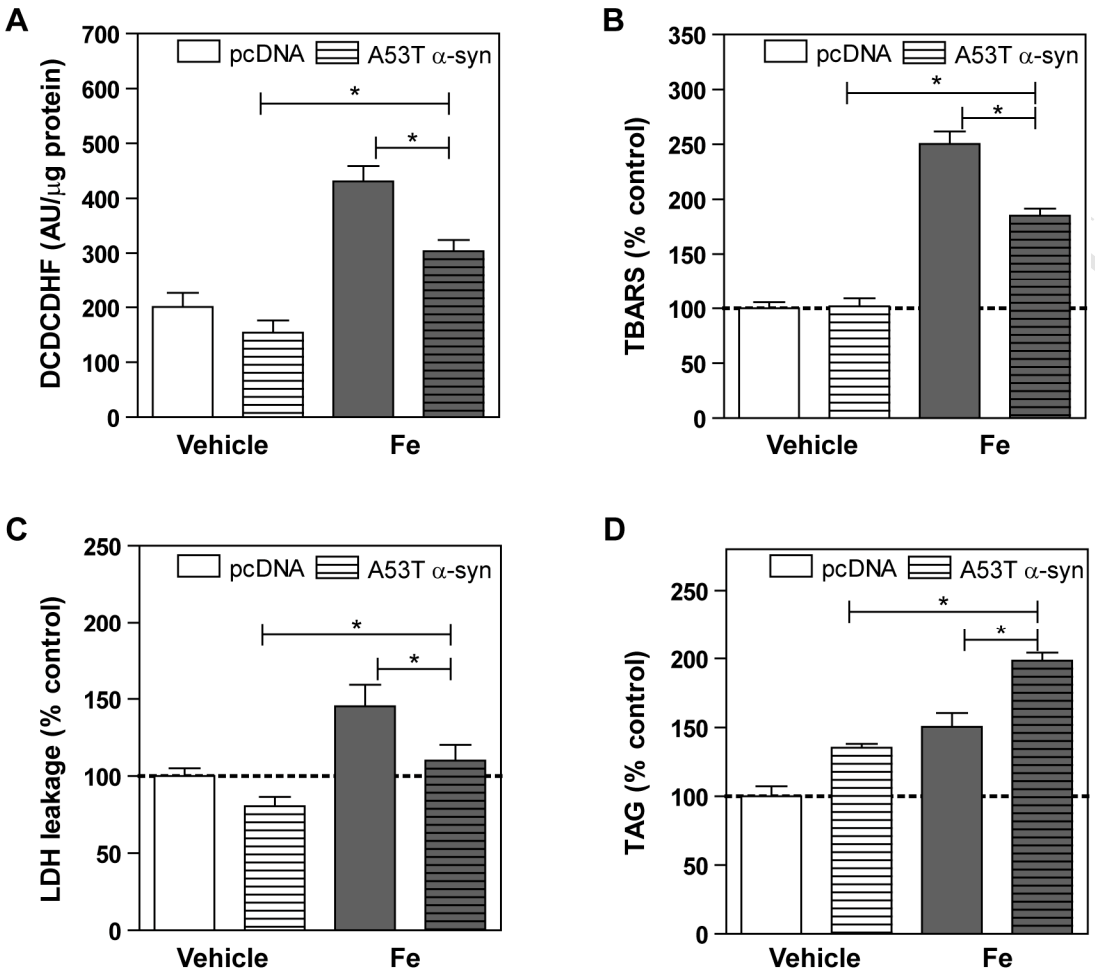

Figure 1

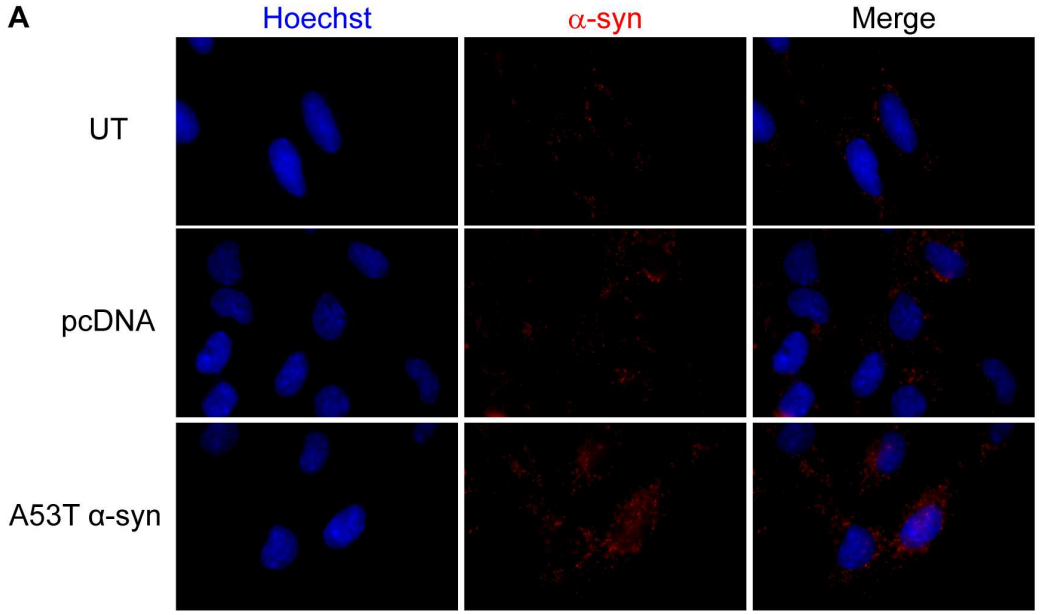
A
Hoechst
α-syn
Merge
UT
pcDNA
A53T α-syn

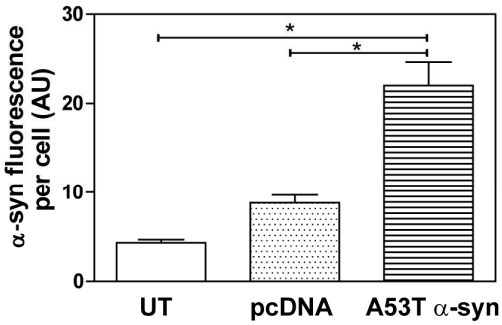
α-syn fluorescence per cell (AU)
30
20
10
0
*
*
UT
pcDNA
A53T α-syn

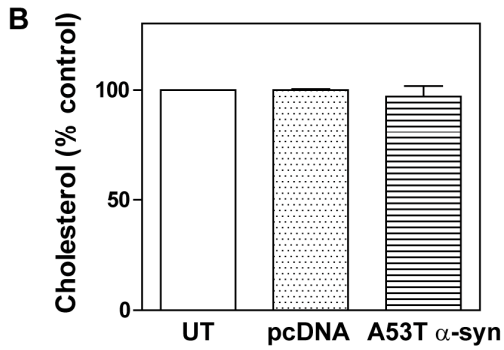
B
Cholesterol (% control)
100
50
0
UT
pcDNA
A53T α-syn

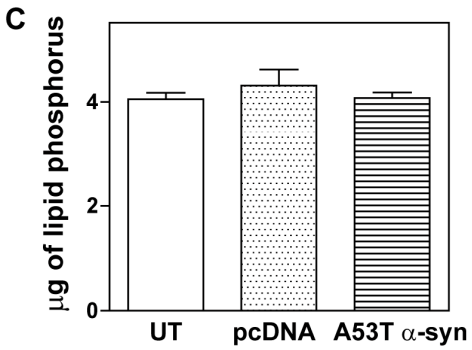
C
μg of lipid phosphorus
4
2
0
UT
pcDNA
A53T α-syn

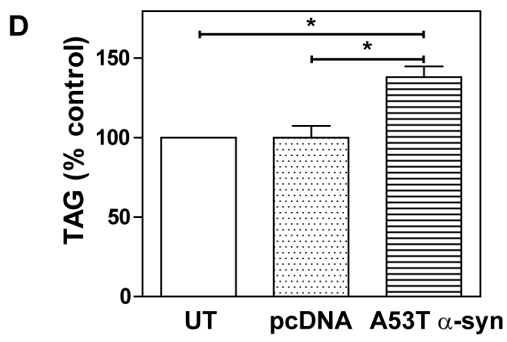
D
TAG (% control)
150
100
50
0
*
*
UT
pcDNA
A53T α-syn

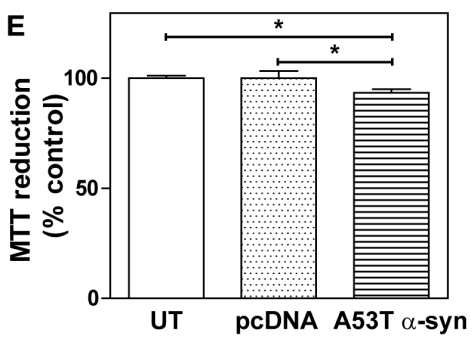
E
MTT reduction (% control)
100
50
0
*
*
UT
pcDNA
A53T α-syn